USE OF SLOPE FAILURES INVENTORY AND CLIMATIC DATA FOR LANDSLIDE SUSCEPTIBILITY, VULNERABILITY, AND RISK MAPPING IN SOUK AHRAS REGION

Abdelouahad EL MEKKI[1], Riheb HADJI[2]
Fehdi CHEMSEDDINE[1]*

[1] Department of Geology, Water and Environment Lab, Tebessa University, Algeria.
[2] Department of Earth Sciences, IAST, Setif 1 University, Algeria.

Abstract: Slope failures (SF) in mountainous terrain often occur during or after heavy rainstorms, resulting in the loss of life and damage to the natural and/or built environment. Assessing areas susceptible to SF is essential for land use planning in threatened areas. This article presents an didactic based-analysis of the potential contribution to geo-spatial approaches for predicting SF qualitative exposure in mountainous environment. Its main aim is to assess the impact of the geologic, geomorphic, rainstorms, and anthropogenic factors in the initiation of SF in Zaarouria region. 219 events (1996–2016) were inventoried through images interpretation and field surveys and were compared to the physical parameters of the terrain to give a SF susceptibility index value using a simplified model. Vulnerability and risk maps are also established. The Standard deviation classification was used to delineate various suscepti-bility, vulnerability and risk zones, namely, nil, low, moderate and high. Field data on SF were employed to evaluate and validate the susceptibility zonation map. The results of this study demonstrate that SF are largely governed not only by geoenvironmental conditions but also by human activities, mainly roads and construction.

Keywords: *risk, GIS, vulnerability, slope failures, landslide susceptibility*

1. INTRODUCTION

Natural hazards are present in all continents, and play an important role in the landscapes evolution. In many countries they pose a serious threat to the population (Hadji et al. 2013). Between all morphogenetic phenomenon, slope failures (SF) are the most injurious to man and his physical environment in the Northeastern areas of Algeria (Guettouche et al. 2013; Bourenane et al. 2014; Gadri et al. 2015; Mokadem et al. 2016; Zahri et al. 2016; Mouici et al. 2017; Achour et al. 2017; Dahoua et al. 2017). They affect and damage mainly the transportation infrastructures. Every year, the same types of instabilities occurs, especially after the winter rainstorms. This situation has become a real constraint to any development in this region. The area chosen for our study suffers from the recurrence of SF of several types (Hadji et al. 2017). This situation is aggravated by the glaring lack of a regulatory mapping providing a general framework for the SF risk management. The investigation method depends on several parameters such as: the work scale, the physical characteristics of the terrain, the data availability, the administrative management framework and the existing cartographic background. These methodes are divided between direct and indirect approaches (Grozavu et al. 2013; Hadji et al. 2016). The adopted approach by our research is based on an expert statistical model defining the relationship between SF and their causative factors. This modeling allows for a reasonable assessment of the SF threats encountered by the study area using thematic susceptibility, vulnerability and risk maps. Such documents makes it possible to identify potentially unstable areas, requiring special treatment during land-use planning operations. The fluctuation of meteorologic variables such as precipitations, snow melting, and temperature changes influence the slopes equilibrium and may cause landslides. At this stage, no consensual evidence exists on the real effects of climate change on the geo-hydrological hazards. The landslides occurrence remains a subject of scientific debate. Their precise estimates is complicated to determine, and to predict (El Gayar and Hamed 2017). However there is the need to evaluate how climate variability affect landslide hazards. Several reseachs have argued that their changes influences slope stability at different temporal and geographical scales (Gariano and Guzzetti 2016; Besser et al. 2017; 2018). Guzzetti et al. (2005) agree that the frequency, probability, density and size of landslides increases significantly in a decadal period. However the intrinsic characteristics of the slope materials do not change in the considered period.

2. STUDY AREA CHARACTERISTICS

The study area occupies the central part of Souk Ahras province, between 36°06'04.97" to 36°19'26.69"N latitudes, and 07°51'11.38" to 8°04'19.52"E longi-

tudes. It includes two municipalities Zaarouria and Souk Ahras and covers a total area of 206.145 km^2 (Fig. 1). It is bounded from the North by Machroha and Ouled Driss, from the East by Ouilen and Mrahna, from the West by Hanancha and Tifech and from the South by Dréa and Taoura municipality. The residential population is estimated at 166,493 inhabitants (ONS 2008). Its climate is semi-arid with a warm and dry summer and a cold and humid winter. The average precipitation is around 840.74 mm/year (Hadji et al. 2014a; Hamad et al. 2018). Its altitudes vary between 480 m and 1090 m a.s.l. Two major structural directions characterize the region; an NE–SW Atlasic direction and an NW–SE to WNW–ESE Miocene tectonic bound. The hydrographic network is well developed, and is represented by temporary streams on the slopes flanks, plunging into the Medjerda valley (Hamed et al. 2014; 2017).

Fig. 1. Geographic location of the study area

3. METHODOLOGY

3.1. FACTORS DATABASE

Slope faillures (SF) involve flowing, sliding, toppling, falling, or spreading, and many landslides exhibit a combination of different types of movements (Rouabhia et al. 2012). The Landslides of the study area are predominantly mudslides and both rotational and translational slides affecting clayey and silty–clayey formations. Precipitation that saturates slopes with water is the main triggering factor of these mass wasting (Hadji et al., 2014b). In some areas, human actions may also triggers landslides. A chronology of landslides, has been reconstructed from technical reports, field surveys, Sentinel-2 + Landsat8 satellite images and Aerial View – Bing Maps for rapid operational inventory mapping. The precipitation conditions responsible for triggering and reactivating landslides have been deduced by analysis of rainfall records. The correlation between SF and precipitations show a strong relationship between rainfall events and the occurrence of landslides.

Even seismic stresses and anthropogenic activities can also trigger SF. The visual-interpretation satellite images and aerial photographs allowed us to make an inventory of 219 events (1996–2016), (Fig. 3a). Landslides were detected by interpreting all the

typical geomorphic characteristics of landslide scars. Field reconnaissance followed this operation to confirm and identify the recognized SF. Different measurements have been made to specify the local factors controlling the dynamics of these instabilities. These landslides were then classified and sorted out based on their modes of occurrence with respect to the existing landslide inventory.
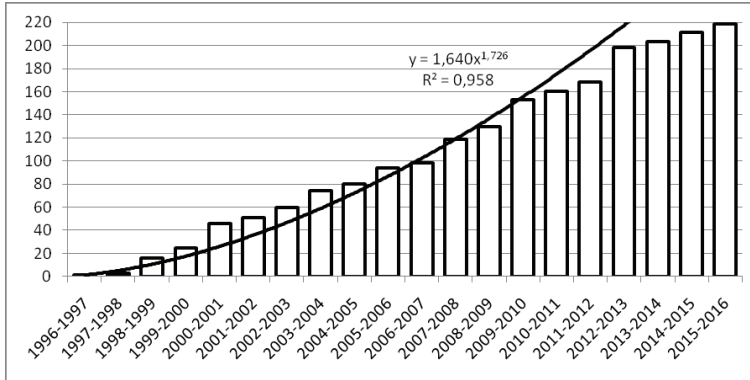

Fig. 2. Landslide occurrence between 1996 and 2016

The inventoried landslides displays many behaviors styles, including long-term creep, sudden brutal movement with no creep phase. Rotational landslide are caracterised by the downward and outward movement of a mass on top of a concave upward failure surface. Whereas ranslational landslide are caracterised by a mass that slides downward and outward on top of an inclined planar surface.

In this study, at first, the total landslides observed in the study area were split into two parts (70%) landslides were randomly selected from the total 219 landslides as the training data and the remaining (30%) landslides were kept for validation propose. Then the rate curves were obtained by comparing the landslide training data and validation data with the susceptibility maps and the areas under the curve were calculated.

The lithology and lineament were digitized on the basis of three geological map (namely Souk Ahras N° 77, M'daourouch N° 100 and Taoura N° 101, in 1/50000 scale). All formations were vectorized in polygons. An attribute database has been created, containing for each lithological unit the facies name, age and symbol, etc. The facies renowned for their weakness to SF are very abundant in the study area. Pliocene red clays, Eocene yellow marls, Cretaceous clay and Triassic gypsum-clay constitutes the majority of the study area facies (Fig. 3b). Lineaments were separately digitized into polylines from the same cartographic background. They have been integrated into the modeling by adopting buffers of: <500 m, 500 to 1000 m and >1000 m around the faults axis (Fig. 3c).

Slope is the main predisposing factor of SF (Pradhan and Lee 2010). It ranges in the study area between 0° and 79°, with an average of about 8.34° and a standard de-

viation of 7.26° (Fig. 3d). On the basis of field observations, the slope map was ranged in five classes: <5°, [5–10°], [10–20°], [20–30°] and ≥30°. The first and the second classes are hardly favorable to the SF genesis. The third class is not very stable; the fourth shows clear indices of instability. Finally, most of the slopes belonging to the fifth class are almost unstable.

The elevation map of the study area was subdivided into seven hypsometric belts between 480 and 1090 m (Fig. 3e). The highest elevations (1000–1090 m) are located on the peaks of Jebel Chouga and Jebel Zaarouria and occupy 1.776 km². The lowest elevations (480–500 m) are concentrated in the valey of Medjerda wady with 1.041 km². The 700–800 m class has the largest area, with 75.526 km².

The aspect map expresses the slopes orientation toward the North (Fig. 3f). It reveals the shadiest slopes and therefore the most humid ones (Pourghasemi et al. 2012). This moisture has a positive predisposition to sliding. Thus, slope, elevation and slope orientation map was prepared using the DEM (30 × 30 m).
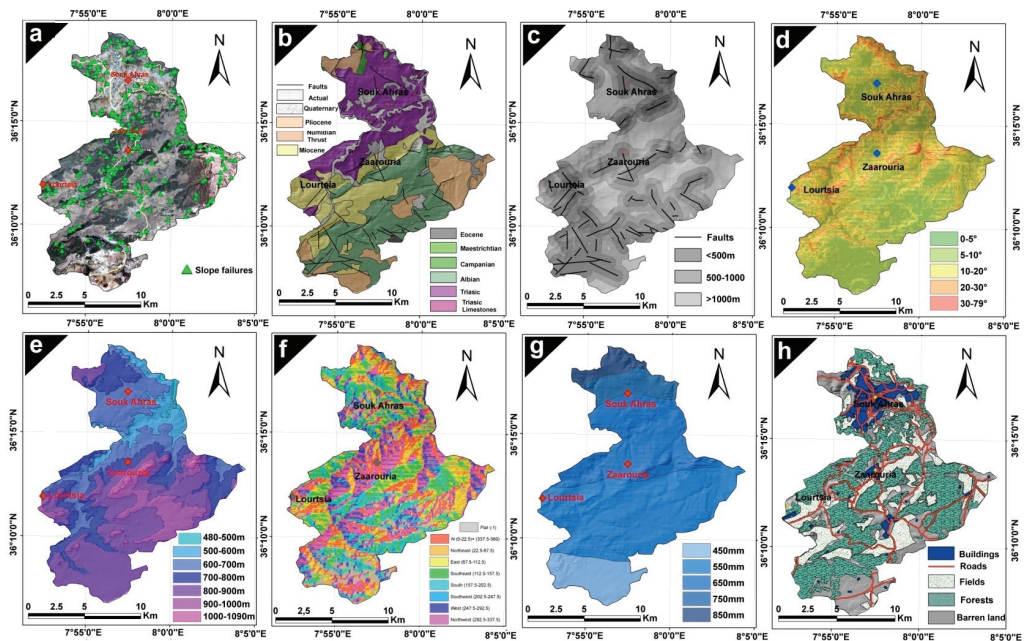

Fig. 3. a – SF inventory map of the study area, b – simplified lithologic map of the study area,
c – buffer lineaments map of the study area, d – slope map of the study area,
e – elevation map of the study area, f – aspect map of the study area,
g – precipitations map of the study area, h – landuse map of the study area.

Rainfalls are well known for their role in triggering SF (Lee and Pradhan 2007). The precipitation map of the study area was clipped from the rainfall map of Northern

Algeria (Awadallah and Foda 2011). The resulting map (Fig. 3g) has five classes: the class <550 mm (23.913 km^2) covers the extreme South of the study area, the isohyet [550, 650 mm] (95.082 km^2) is top of the previous one; The class [650, 750 mm] (62,013 km^2) is in the middle of the study area; That of [650, 750 mm] (15,923 km^2) to its North while the class >750 mm: (9.215 km^2) is in the extreme North.

Land use of the study area was mapped using a multi-source database with satellite imagery, topographic maps supplemented by fieldwork. This information has been used to digitize and index road networks, buildings, agricultural fields, forests and bare land (Fig. 3h). The roads were integrated into the modeling by adopting buffers of <25 m, from 25 to 50 m and >50 m around the road and rail axes.

3.2. METHODOLOGY

3.2.1. SUSCEPTIBILITY MAPPING

The susceptibility assessment follows four steps:
- The SF inventory based on satellite images interpretation by using Landsat8 images;
- The mapping of causative factors, which are supposed to be responsible for the appearance of SF in the study area;
- The estimation of the relative importance of each categorical variable involved in the SF genesis;
- The SF susceptibility assessment in the study area and the validation of the model.

All layers were rasterized in the same pixel format (5 × 5 m). Susceptibility index were established by the overlaying of each factor separately on the SF inventory map. Buffer zones have been established around linear themes such as faults, roads and the hydrographic network to allow their integration in modeling. Geological information (lithology and fault buffers (A, B)) Land use (road buffers, buildings, forests and fields (C)); Morphological data (altitude, slope classes and aspect (D, E, F)) and environmental data (rainfall, hydrographic network buffers, and earthquakes (the latter factor is mono-zonal)) Are introduced into the evaluation of the susceptibility map. The susceptibility index (H_{ji}, = decimal number between 0 and 1) interpreting the relationship between the spatial distribution of SF and the different elementary classes of the causative factors were calculated. Several weighting trials (W_j = integer between 1 and 4) interpreting the importance of each factor in the genesis of slope breaks in the study area have been tested. 25 Receiver Operating Characteristic (ROC) curves were tested for various weight combinations (by integrating the 30% (66 cases) of events omitted by a random process). The best combination has been selected for generating the susceptibility map of the study area. The value of the SF susceptibility at each point of the 8234175 pixels is calculated according to the following equation:

$$\text{Susceptibility} = \frac{\sum_{j=1}^{9}[W_j, H_{ji}]}{\sum_{j=1}^{9}W_j} \qquad (1)$$

The ROC curve of the selected model shows the largest area under the curve AUC = 0.79. This value is judged by our study as quite satisfactory (Fig. 4 a).
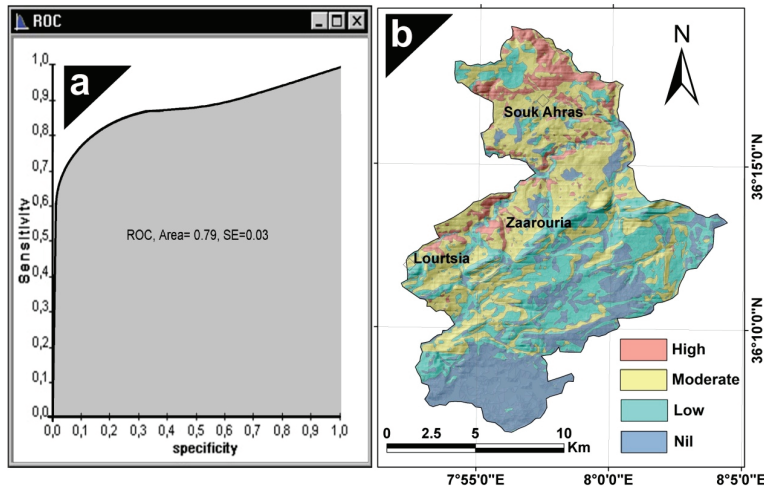

Fig. 4. a – ROC curve of the retained model (AUC = 0.79),
b – SF susceptibility map of the study area

In the adopted model, a maximum weighting aqual to four (W_F, W_I and $W_A = 4$) was attributed to slope, precipitations and lithology, due to their primary role (high correlation) in the genesis and the initiation of the phenomenon. A minimum weight equal to one (W_B, W_D and $W_E = 1$) is assigned to the fault, elevation and aspect layer. All other layers are assigned a weighting equal to two ($W_{C, J, K} = 2$). The resulting map was prioritized into four qualitative classes using the Standard Deviation classifier, which resulted in the final SF susceptibility map of the study area. It is divided to nil 23.38% (48.192 km^2), low 31.53% (64.994 km^2), moderate 36.97% (76.223 km^2) and High class 8.12% (16.736 km^2) (Fig. 4b).

3.2.2. VULNERABILITY MAPPING

In order to determine the vulnerability of property and people to SF, a typology of the territory's components in transport infrastructures, buildings and functionalities has been carried out. Topographic maps, satellite images and feld work were used to ana-lyze these themes. Loss index values (Ip = decimal number between 0 and 1) are assigned to the various elements to estimate damage, loss or other adverse effects to

those attributes valued by mankind. The vulnerability map was elaborated by modeling the consequences account values of four themes represented by the building, road, agricultural fields and the forests; Estimating the physical injuries, structural damages, and functional disorders related to a SF possible occurrence.

Several approach considers that main damage to the exposed elements is structural, corporal and operational (Leone et al. 1996). Vulnerability is the degree of loss of an element within the landslideaffected area (Fell 1994). The type and the quality of the buildings is a criterion of structural and corporal vulnerability. If this criterion is high, the concerned area is more vulnerable. In our work we have attributed to this theme a maximum loss index ($Ip = 1$) (Fig. 5a).

The importance of a road and the number of its users is an indicator of vulnerability. If a SF cuts off a road and makes it temporarily obstructed, the The traveler on this axis will have to take another path. The value of the associated loss index quantifies the difficulties caused by such changes. National highways (RN) and railway lines (CF) have been assigned a maximum loss index ($Ip = 1$), (due to the irreplaceability of these axes). Whereas for provincial roads (*CW*) it is rather a moderate value ($Ip = 0.5$) (because of the possible alternatives for the users of these roads in the event of a cut-off of these axes) (Fig. 5b).

In addition to the previous themes, it seems necessary to interpret the land occupation in terms of agricultural fields and forests. These themes have an economic interest (agriculture) and tourism (mountain hiking) for the citizens of the region. A moderate loss index ($Ip = 0.5$) was assigned to the fields (Fig 5c) and low ($Ip = 0.25$) to the forests (Fig. 5d). A nil loss index was assigned to the bare lands.
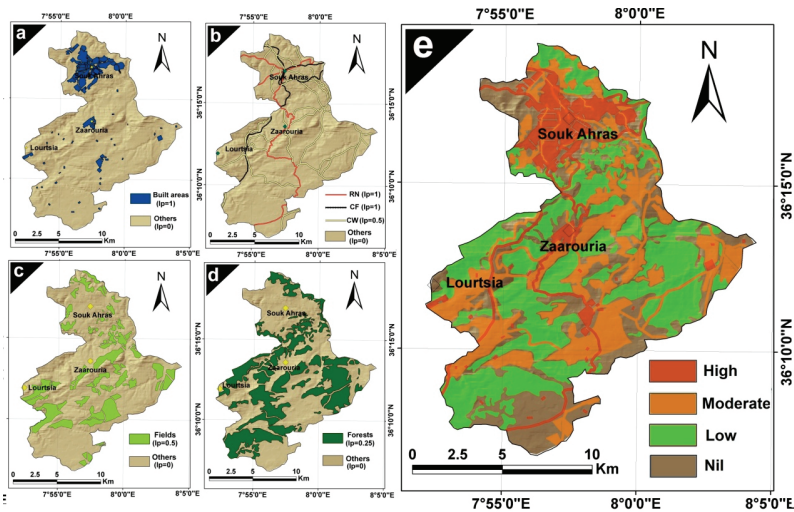

Fig. 5. a – build area map of the study area, b – roads network, c – agricultural fields, d – forest map, e – SF vulnerability map of the study area

The maximum value of the loss indexes of the different themes was retained. The assembly of these values gave a map of the global vulnerability indices. The results were harmonized on a scale of 0 to 1 and then hierarchized with the standard deviation method into four vulnerability cartographic classes, Nil = 26.41%, Low = 36.81%; Moderate = 26.83% and High = 9.95% (Fig. 5e).

3.2.3. RISK MAPPING

The risk is the intersection of two components: the likelihood of something adverse happening and the consequences if it does (Crozier and Glade 2006). The level of risk thus results from the combination of susceptibility with the value of the elements at risk by way of their vulnerability. For the assessment of the SF risk to property and people, susceptibility and vulnerability categories, are translated into risk classes using a pairwise matrix (Fig. 6, Table 1) (Ko et al. 2004).
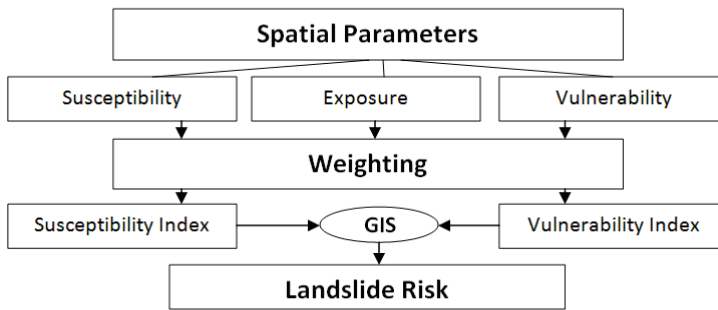

Fig. 6. Methodological flowchart of the study

It was determined that a high risk resulted from the combination of a high suscepti-bility with a high or moderate vulnerability, etc. The application of this table makes it possible to obtain a total risk map of the studied territories (Fig. 7). It is divided into four hierarchical risk classes: Nil = 51.33%, Low = 23.51%, Moderate = 17.90% and High = 7.26%.

Table 1. Qualification matrix of the cartographic risk classes

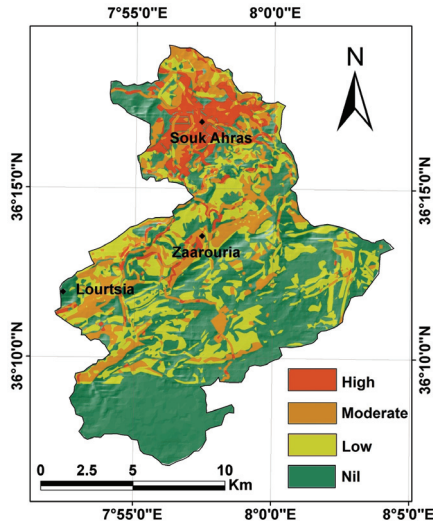| Susceptibility / Vulnerability	High	Moderate	Low	Nil
High	High	High	Moderate	Nil
Moderate	High	Moderate	Low	Nil
Low	Moderate	Low	Low	Nil
Nil	Nil	Nil	Nil	Nil

Fig. 7. SF risk map of the study area

4. RESULTS AND DISCUSSIONS

Our simplified approach allowed the comprehensive study of SF susceptibilitys, vulnerability and risk in the Zaarouria and Souk Ahras region. The AUC validated the model at 79%. The standard deviation method was used to prioritize susceptibility and vulnerability maps in four classes each. The nil susceptibility class covers 48.192 km^2 of the total 206.145 km^2 of the study area. It is concentrated in the South part, and is caracterized by gentle slopes. The low-susceptibility class is 64.994 km^2 and is concentrated in the middle of the study area with little rainfall. The moderate susceptibility stretches over 76.223 km^2 and is spread over Triassic terrains in the vicinity of the mountainous reliefs in the middle and North of the study area. The high susceptibility class covers approximately 16.736 km^2. In this zone, slopes and precipitations are importants. The geological formations are represented by sensitive lithologies to sliding.

The Nil vulnerability class covers 54.443 km^2 and dominates the extreme south of the study area, it is represented mainly by bare lands. The low vulnerability class spreads over most of the study area and covers 75.882 km^2. It is represented by poorly maintained forests. The moderate one is presented by the agricultural fields and covers 55.308 km^2, while the high vulnerability class includes the building national roads and rail axes. It is concentrated in the chief town territory and covers 20.512 km^2.

The nil risk class covers 105.814 km^2. It is concentrated on the plains and alluvial terraces of the southern part of the study area where the susceptibility and vulnerabil-

ity values are low to nil. The low risk class 48.465 km^2 occupies the middle of the study area side by side with the moderate risk class 36.9 km^2. The high risk class is concentrated in the North of the study area where the values of the susceptibility and the vulnerability are high, it covers 14.966 km^2. Unfortunately this class coincides with the concentration of the main issues.

The most important predisposing factors of the study area to SF are lithology and slopes, and the main triggering factor is precipitations. The other factors do not have the same importance. The distribution of SF susceptibility and risk is in perfect agreement with our field observations. This demonstrates that the approach taken by our research can provide a reasonable estimation of the phenomenon in the study area. Some results seem unexpected! Thus, the SF are more abundant on slopes greater than 30 °! This is explained by the lithological and neotectonic role of the Triasic diapir.

5. CONCLUSIONS AND RECOMMENDATION

This research demonstrates the performance of GIS-based approaches in assessing SF risk from a three-step process where risk is identified and mapped by combining susceptibility and vulnerability.

The SF inventory (1.06 events/km^2) allowed to assess qualitatively and quantitatively the magnitude of these instabilities: quantitatively by means of an interpretation of multi-date satellite images; And qualitatively by determining the signs of instability on the slopes of the study area.

The processing of the selected causal factors (interpreting the geological context, geomorphological conditions, hydrographic network, precipitations, and land use, etc.) allowed to model the spatio-temporal effects of the various categorical variables involved in the genesis of SF. The Raster linear summation made it possible to calculate SF susceptibility, vulnerability and risk maps.

The chief town of the province (where people the and property are concentrated) belong to a highly susceptible terrains to SF. This situation requires the promotion of a geo-risk culture among population and decision-makers.

This method can be used as an referential information system for managing SF risk in the study area. It can be replicated by other studies to estimate the susceptibility, vulnerability and risk of SF in similar environments.

REFERENCES

ACHOUR Y., BOUMEZBEUR A., HADJI R. et al., 2017, *Landslide susceptibility mapping using analytic hierarchy process and information value methods along a highway road section in Constantine, Algeria*, Arab J. Geosci., 10, 194.

AWADALLAH A.G., FODA R., 2011, *Approche statistique régionale pour l'estimation des caractéristiques pluviométriques: Etude de cas au Nord Est de l'Algérie*, Canadian Journal of Civil Engineering, 38 (10), 1060–1071.

BESSER H., MOKADEM N., REDHAOUNIA B., HADJI R., HAMAD A., HAMED Y., 2018, *Groundwater mixing and geochemical assessment of low-enthalpy resources in the geothermal field of southwestern Tunisia*, Euro-Mediterranean Journal for Environmental Integration, 3 (1), 16.

BESSER H., MOKADEM N., REDHOUANIA B., RHIMI N., KHLIFI F., AYADI Y., ... and HAMED Y., 2017, *GIS-based evaluation of groundwater quality and estimation of soil salinization and land degradation risks in an arid Mediterranean site (SW Tunisia)*, Arabian Journal of Geosciences, 10 (16), 350.

BOURENANE H., BOUHADAD Y., GUETTOUCHE M.S., BRAHAM M., 2015, *GIS-based landslide susceptibility zonation using bivariate statistical and expert approaches in the city of Constantine (Northeast Algeria)*, Bulletin of Engineering Geology and the Environment, 74 (2), 337–355.

CROZIER M.J., GLADE T., 2006, *Landslide susceptibility and risk: issues, concepts and approach*, Vol. 802, CROZIER.

DAHOUA L., SAVENKO V.Y., HADJI R., 2017, *GIS-based technic for roadside-slope stability assessment: an bivariate approach for A1 East-west highway, North Algeria*, Mining Science, 24, 81–91.

EL GAYAR A., HAMED Y., November 2017, *Climate Change and Water Resources Management in Arab Countries*. In: Euro-Mediterranean Conference for Environmental Integration, Springer, Cham., pp. 89–91.

GADRI L., HADJI R., ZAHRI F., BENGHAZI Z., BOUMEZBEUR A., LAID B.M., RAÏS K., 2015, *The quarries edges stability in opencast mines: a case study of the Jebel Onk phosphate mine, NE Algeria*, Arabian Journal of Geosciences, 8 (11), 8987–8997.

GARIANO S.L., GUZZETTI F., 2016, *Landslides in a changing climate*, Earth-Science Reviews, 162, 227–252.

GROZAVU A., PLEŞCAN S., PATRICHE C.V., MĂRGĂRINT M.C., ROŞCA B., 2013, *Landslide susceptibility assessment: GIS application to a complex mountainous environment*. In: The Carpathians: Integrating Nature and Society Towards Sustainability, Springer, Berlin–Heidelberg, pp. 31–44.

GUZZETTI F., REICHENBACH P., CARDINALI M., GALLI M., ARDIZZONE F., 2005, *Probabilistic landslide hazard assessment at the basin scale*, Geomorphology, 72 (1–4), 272–299.

HADJI R., ACHOUR Y., HAMED Y., November 2017, *Using GIS and RS for Slope Movement Susceptibility Mapping: Comparing AHP, LI and LR Methods for the Oued Mellah Basin, NE Algeria*. In: Euro-Mediterranean Conference for Environmental Integration, Springer, Cham., pp. 1853–1856.

HADJI R., CHOUABI A., GADRI L., RAÏS K., HAMED Y., BOUMAZBEUR A., 2016, *Application of linear indexing model and GIS techniques for the slope movement susceptibility modeling in Bousselam upstream basin. Northeast Algeria*, Arabian Journal of Geosciences, 9 (3), 192.

HADJI R., ERRAHMANE BOUMAZBEUR A., LIMANI Y., BAGHEM M., EL MADJID CHOUABI A., DEMDOUM A., 2013, *Geologic, topographic and climatic controls in landslide susceptibility assessment using GIS modeling: a case study of Souk Ahras region, NE Algeria*, Quaternary International, 302, 224–237.

HADJI R., LIMANI Y., DEMDOUM A., 2014b, *Using multivariate approach and GIS applications to predict slope instability susceptibility case study of Machrouha municipality, NE Algeria*. In:, IEEE 2014 1st International Conference on Information and Communication Technologies for Disaster Management (ICT-DM), pp. 1–10.

HADJI R., LIMANI Y., BOUMAZBEUR A.E., DEMDOUM A., ZIGHMI K., ZAHRI F., CHOUABI A., 2014a, *Climate change and its influence on shrinkage–swelling clays susceptibility in a semi-arid zone: a case study of Souk Ahras municipality, NE-Algeria*, Desalination and Water Treatment, 52 (10–12), 2057–2072.

HADJI R., RAIS K., GADRI L., CHOUABI A., HAMED Y., 2017, *Slope failure characteristics and slope movement susceptibility assessment using GIS in a medium scale: a case study from Ouled Driss and Machroha municipalities, Northeast Algeria*, Arabian Journal for Science and Engineering, 42 (1), 281–300.

HAMAD A., BAALI F., HADJI R., ZERROUKI H., BESSER H., MOKADEM N., ... and HAMED Y., 2018, *Hydrogeochemical characterization of water mineralization in Tebessa-Kasserine karst system (Tuniso-Algerian Transboundry basin)*, Euro-Mediterranean Journal for Environmental Integration, 3 (1), 7.

HAMED Y., REDHAOUNIA B., BEN SÂAD A., HADJI R., ZAHRI F., ZIGHMI K., 2017, *Hydrothermal waters from karst aquifer: Case study of the Trozza basin (Central Tunisia)*, Journal of Tethys, 5 (1), 33–44.

HAMED Y., AHMADI R., HADJI R., MOKADEM N., BEN DHIA H., ALI W., 2014, *Groundwater evolution of the Continental Intercalaire aquifer of Southern Tunisia and a part of Southern Algeria: use of geochemical and isotopic indicators*, Desalination and Water Treatment 52 (10–12), 1990–1996.

KO C.K., FLENTJE P., CHOWDHURY R., 2004, *Landslides qualitative susceptibility and risk assessment method and its reliability*, Bulletin of Engineering Geology and the Environment, 63 (2), 149–165.

LEE S., PRADHAN B., 2007, *Landslide susceptibility mapping at Selangor, Malaysia using frequency ratio and logistic regression models*, Landslides, 4 (1), 33–41.

MOKADEM N., DEMDOUM A., HAMED Y., BOURI S., HADJI R., BOYCE A., LAOUAR R., SAAD A., 2016, *Hydrogeochemical and stable isotope data of groundwater of a multi-aquifer system: Northern Gafsa basin e Central Tunisia*, Journal of African Earth Sciences, 114, 174–191.

MOUICI R., BAALI F., HADJI R., BOUBAYA D., AUDRA P., FEHDI C.É., ... and ARFIB B., 2017, *Geophysical, Geotechnical, and Speleologic assessment for karst-sinkhole collapse genesis in Cheria plateau (NE Algeria)*, Mining Science, 24, 59–71.

POURGHASEMI H.R., PRADHAN B., GOKCEOGLU C., 2012, *Application of fuzzy logic and analytical hierarchy process (AHP) to landslide susceptibility mapping at Haraz watershed, Iran*, Natural susceptibilitys, 63 (2), 965–996.

PRADHAN B., LEE S., 2010, *Regional landslide susceptibility analysis using back-propagation neural network model at Cameron Highland, Malaysia*, Landslides, 7 (1), 13–30.

ROUABHIA A., DJABRI L., HADJI R., BAALI F., FAHDI Ch., HANNI A., 2012, *Geochemical characterization of groundwater from shallow aquifer surrounding Fetzara Lake NE Algeria*, Arabian Journal of Geosciences, 5 (1), 1–13.

ZAHRI F., BOUKELLOUL M., HADJI R., TALHI K., 2016, *Slope Stability Analysis in Open Pit Mines of Jebel Gustar Career, NE Algeria – A Multi-Steps Approach*, Mining Science, 23, 137–146.